Revista Brasileira de Geofísica
RBGf
Brazilian Journal of Geophysics

Revista Brasileira de Geofísica (2012) 30(1): 81-92

ISSN 0102-261X
www.scielo.br/rbg

GEOELECTRIC DIRECTIONALITY OF A MAGNETOTELLURIC (MT) SURVEY IN THE PARECIS BASIN, BRAZIL

Hans Schmidt Santos[1] and Jean Marie Flexor[2]

Recebido em 18 junho, 2011 / Aceito em 21 maio, 2012
Received on June 18, 2011 / Accepted on May 21, 2012

ABSTRACT. Eighty-eight broadband (0.001-1000 sec) magnetotelluric (MT) soundings have been made along a 500 km profile crossing the Parecis Basin (Mato Grosso State and Rondônia State, Brazil) in a direction almost perpendicular to the main geological lineaments. The two-dimensional inversion (2-D) of MT data (constrained by well-log resistivity data) allowed to estimate the distribution of the conductivity. For the inversion procedure, the impedance tensors were rotated by an angle of 130° (± 10°) (~ E-W) measured clockwise from the geographic north according to the dominant geological trend estimated of the Parecis Basin. Accurate interpretation of MT data requires understanding the dimensionality and directionality conditions that must be satisfied by the properties of the impedance tensor. However, due to the usual presence of shallow, small-scale galvanic bodies which distort the responses, the regional scale structures can be masked. In order to verify if an average geoelectric strike can be compatible with the basin's geological strike, a procedure of decomposition of MT impedance tensor for a set of 36 MT soundings along the profile was applied. The results show the angular distribution of the geoelectric strike. The observed departures from an average angle value are explained both in terms of geotectonic structures of the Parecis Basin and of their influences in the geoelectric anisotropy. From a three-dimensional model of the basement topography based on downward continuation of gravity field constrained by spectral estimates of depth to magnetic sources, it is shown that the most regular strike angle distributions correspond to the deepest sedimentary structures: Caiabis, Pimenta Bueno and Colorado grabens. In the interface regions, we expect anisotropy distorting strongly the regional impedance tensor.

Keywords: magnetotelluric method, basin, geoelectric directionality.

RESUMO. Oitenta e oito sondagens magnetotelúricas de banda larga (0,001-1000 s) foram realizadas ao longo de um perfil de 500 km cruzando a Bacia de Parecis (Mato Grosso e Rondônia) em uma direção quase perpendicular aos principais lineamentos geológicos. A inversão em duas dimensões (2-D) dos dados MT (vinculada aos dados de resistividade do poço) permitiu imagear a distribuição da condutividade. Para o procedimento de inversão, os tensores de impedância foram girados de um ângulo de 130° (± 10°) (~ E-W) de acordo com a direção estimada do lineamento geológico dominante da Bacia dos Parecis. Uma interpretação adequada dos dados MT requer a compreensão das condições de dimensionalidade e direcionalidade que devem ser satisfeitas pelas propriedades do tensor de impedância. Contudo, devido à presença de heterogeneidades galvânicas rasas que distorcem as respostas, as estruturas em escala regional podem ser mascaradas. A fim de verificar se o *strike* geoelétrico é compatível com a escolha prévia do *strike* geológico, aplicou-se um procedimento de decomposição do tensor impedância MT para um conjunto de 36 sondagens MT no perfil. Os resultados mostram a distribuição dos ângulos de *strike* geolelétrico. Os desvios observados de um valor médio do ângulo são investigados em termos de estruturas geotectônicas da Bacia dos Parecis e suas influências nas anisotropias geoelétricas. De um modelo tridimensional da topografia do embasamento baseado na continuação para baixo do campo de gravidade vinculado por estimativas espectrais de profundidade por fontes magnéticas, mostra-se que as distribuições mais regulares do ângulo de *strike* correspondem às estruturas mais profundas: grábens de Caiabis, Pimenta Bueno e Colorado. Nas regiões de interface, espera-se anisotropia distorcendo o tensor de impedância regional.

Palavras-chave: método magnetotelúrico, bacia, direcionalidade geoelétrica.

[1]Postgraduate Program in Geophysics, Observatório Nacional, Rua General José Cristino, 77, Rio de Janeiro, RJ, Brazil. Phone: +55 (22) 2760-6018 – E-mail: hans@on.br

[2]Coordination of Geophysics, Observatório Nacional, Rua General José Cristino 77, Rio de Janeiro, RJ, Brazil. Phone: +55 (21) 2719-7593; Fax: +55 (21) 2704-2322 – E-mail: flexor@on.br

INTRODUCTION

The Parecis Basin, an intracratonic basin of Brazil, is located in the Central-West Region of Brazil covering an area of about 500,000 km^2. It begins southeast of the Rondônia State and crosses the Mato Grosso State to its limits with the Goiás State. It is located between the Solimões and Paraná basins. The Parecis and Paraná basins are part of the set of Brazilian Paleozoic basins related to the sub-Andean depression (Fig. 1).

The Parecis Basin has accumulated nearly 6000 m of sediments of the Paleozoic, Mesozoic and Cenozoic. The sediments are dominantly siliciclastic rocks, including Cretaceous volcanics – flows and dikes. It occupies the southwestern sector of the Amazonian Craton between the mobile belts of Rondônia and Guaporé. It is limited respectively by the Alto Xingu and Rio Guaporé arcs (Fig. 2). Amazonian Craton rocks constitute the basement of the basin comprising metamorphic, metasedimentary and intrusive rocks.

The Parecis Basin is almost entirely covered by airborne (magnetics and gravity) and terrestrial (gravity) geophysical surveys. We performed a magnetotelluric (MT) sounding profile crossing the basin in an $\sim$ N12°E direction. It was assumed a 2-D dimensionality condition with a geoelectric strike of 130° ($\pm$ 10°) measured clockwise from the geographic north (E20°S–40°S direction range) suggested by the central part of the map from the vertical derivative of the magnetic anomaly (Fig. 3) and the tectonic model obtained by Braga & Siqueira (1995) from the data inversion of gravity (Fig. 4). Afterwards, the use of this geoelectric strike was checked by the decomposition of tensor MT data.

The 2-D inversion of the MT profile was performed using a routine developed by Rodi & Mackie (2001). The routine finds regularized solutions to the two-dimensional inverse problem for MT data using the method of nonlinear conjugate gradients. The forward model simulations were computed using finite difference equations generated by network analogs to Maxwell's equations. The algorithm inverts a user-defined 2-D mesh of resistivity blocks, extending laterally and downwards beyond the central detailed zone, and incorporating topography (Fig. 5).

This inversion procedure was constrained by using well-logging resistivity data (exploratory well 2-SM-1-MT, Fig. 2).

METHOD

The magnetotelluric (MT) method uses natural EM fields measured at the Earth's surface to estimate the subsurface electrical resistivity. Amplitude, phase and directional relations between the electric field $\mathbf{E}$ and the magnetic field $\mathbf{H}$ intensities are connected by the 2×2 response impedance tensor $\tilde{\mathbf{Z}}$

$$\mathbf{E} = \tilde{\mathbf{Z}} \cdot \mathbf{H}$$

and $\tilde{\mathbf{Z}}$ is obtained by robust estimation from the recorded time series of $\mathbf{E}$ and $\mathbf{H}$ in the Fourier domain:

$$\left\langle \tilde{\mathbf{Z}}(\boldsymbol{\omega}) \right\rangle = \left\langle \left(\mathbf{E}(\boldsymbol{\omega})\mathbf{H}(\boldsymbol{\omega})^{\mathbf{T}}\right) \right\rangle \left\langle \left(\mathbf{H}(\boldsymbol{\omega})\mathbf{H}(\boldsymbol{\omega})^{\mathbf{T}}\right)^{-1} \right\rangle \quad (1)$$

where $\mathbf{T}$ is the Hermitian transpose and the quantities in brackets are cross-powers and auto-powers of $\mathbf{E}$ and $\mathbf{H}$. A 2-D dimensionality condition (i.e. the existence of a geoelectric strike) is described by the rotation relations for the impedance tensor

$$\begin{aligned} \tilde{\mathbf{Z}}_{\mathrm{obs}}(\theta_0) &= \mathbf{R}(\theta_0)\tilde{\mathbf{Z}}_{\mathbf{2D}}\mathbf{R}^{\mathbf{T}}(\theta_0) \\ &= \begin{pmatrix} \cos\theta_0 & -\sin\theta_0 \\ \sin\theta_0 & \cos\theta_0 \end{pmatrix} \begin{pmatrix} 0 & Z_{xy} \\ Z_{yx} & 0 \end{pmatrix} \\ &\quad \times \begin{pmatrix} \cos\theta_0 & \sin\theta_0 \\ -\sin\theta_0 & \cos\theta_0 \end{pmatrix} \end{aligned} \quad (2)$$

where $\mathbf{Z}_{\mathrm{obs}}$ is the observed impedance at the sounding station, $\mathbf{R}$ is a rotation tensor and $\mathbf{Z}_{2\mathrm{D}}$ is the impedance rotated to the strike direction θ_0 measured from the geographic north. The corresponding field rotations are given by

$$\begin{cases} \mathbf{E}_{\mathrm{x}}(\theta) = \mathbf{Z}_{\mathrm{xy}}\mathbf{H}_{\mathrm{y}}(\theta), & \text{TE mode} \\ \mathbf{E}_{\mathrm{y}}(\theta) = \mathbf{Z}_{\mathrm{yx}}\mathbf{H}_{\mathrm{x}}(\theta), & \text{TM mode} \end{cases} \quad (3)$$

The strike direction θ_0 can be found by differentiating $\mathbf{Z}$ with respect to θ in order to give an angle θ_0 which maximizes or minimizes $|\mathbf{Z}'_{\mathrm{xy}}(\theta_0)|^2 + |\mathbf{Z}'_{\mathrm{yx}}(\theta_0)|^2$ for all frequencies giving (Vozoff, 1991):

$$\mathbf{4}\theta_0 = \arctan \frac{\left[(\mathbf{Z_{xx}} - \mathbf{Z_{yy}})(\mathbf{Z_{xy}} + \mathbf{Z_{yx}})^* + (\mathbf{Z_{xx}} - \mathbf{Z_{yy}})^*(\mathbf{Z_{xy}} + \mathbf{Z_{yx}})\right]}{|\mathbf{Z_{xx}} - \mathbf{Z_{yy}}|^{\mathbf{2}} - |\mathbf{Z_{xy}} + \mathbf{Z_{yx}}|^{\mathbf{2}}} \quad (4)$$

This leaves four possible solutions or two strike directions with a $\pi/2$ ambiguity which can be solved from independent information (vertical magnetic data – tipper strike) or from geologic insights. The tipper is a MT quantity which depends on the vertical component of the magnetic intensity $\mathbf{H_z}$. This component is $\approx \mathbf{0}$ except near lateral conductivity changes (2-D situations). The tipper $\mathbf{T}$ gives a relationship between $\mathbf{H_z}$ + and the horizontal magnetic components: $\mathbf{H_z} = \mathbf{T_x}\mathbf{H_x} + \mathbf{T_y}\mathbf{H_y}$. For a 2-D structure with strike in the x' direction, in those coordinates, the tipper $\mathbf{T}$ reduces to $\mathbf{H_z} = \mathbf{T_y}\mathbf{H_{y'}}$ (4a). This x' direction corresponds to the tipper strike angle (Vozoff, 1991).

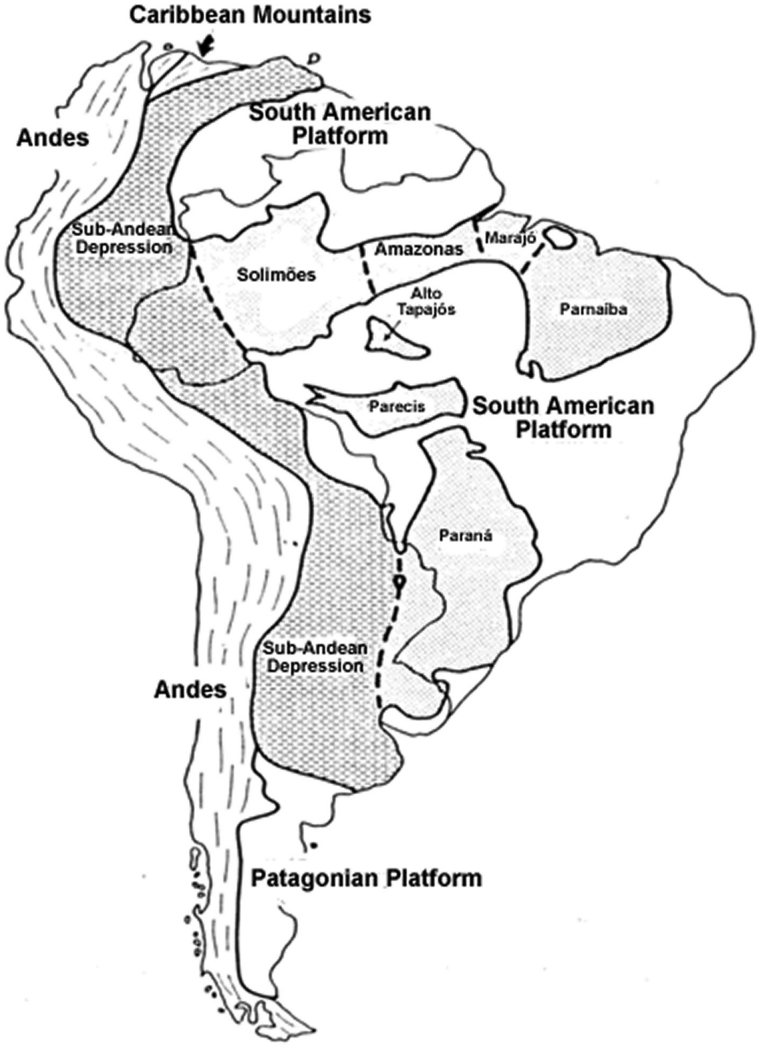

Figure 1 – Paleozoic basins of Brazil and their relations with the Andean region (Siqueira, 1989).

CORRECTION OF STATIC SHIFT

Static shift can be caused by conductivity discontinuities which brings about local distortion of the amplitudes of electric fields. This effect causes impedance magnitudes to be enhanced or diminished by scaling factors. The presence of static shift is realized in data whose apparent resistivities are shifted relative to each other; but impedance phases remain together. Static shift is a galvanic effect which produces a constant vertical displacement among the apparent resistivity curves regardless of frequency (Fig. 6). They are more frequent in highly resistive environments. Where small-scale conductivity heterogeneities have an effect on electric fields. This type of distortion can lead to a misinterpretation of the depths associated with resistivities.

The static shift was corrected by using TDEM (Time Domain Electromagnetic – Transient) resistivity measurements. The TDEM measurement was a tool used for static shift correction according to the methodology suggested by Sternberg et al. (1988). It corrects the displacement of the curves of apparent resistivity MT data by basing the curves of apparent resistivity data TDEM (Figs. 7 and 8).

DECOMPOSITION OF MT IMPEDANCE TENSOR

2-D conductive structure has an impedance tensor described by Equation (2). However, small local inhomogeneities will produce a galvanic distortion independent of the frequency of the regional telluric currents. The observed impedance tensor can be decomposed following the Groom & Bailey (1989) factorization. In this case, the observed impedance tensor is written as

$$\tilde{\mathbf{Z}}_{\mathbf{obs}} = \mathbf{R}\mathbf{C}\tilde{\mathbf{Z}}_{\mathbf{2D}}\mathbf{R}^{\mathbf{T}} \qquad (5)$$

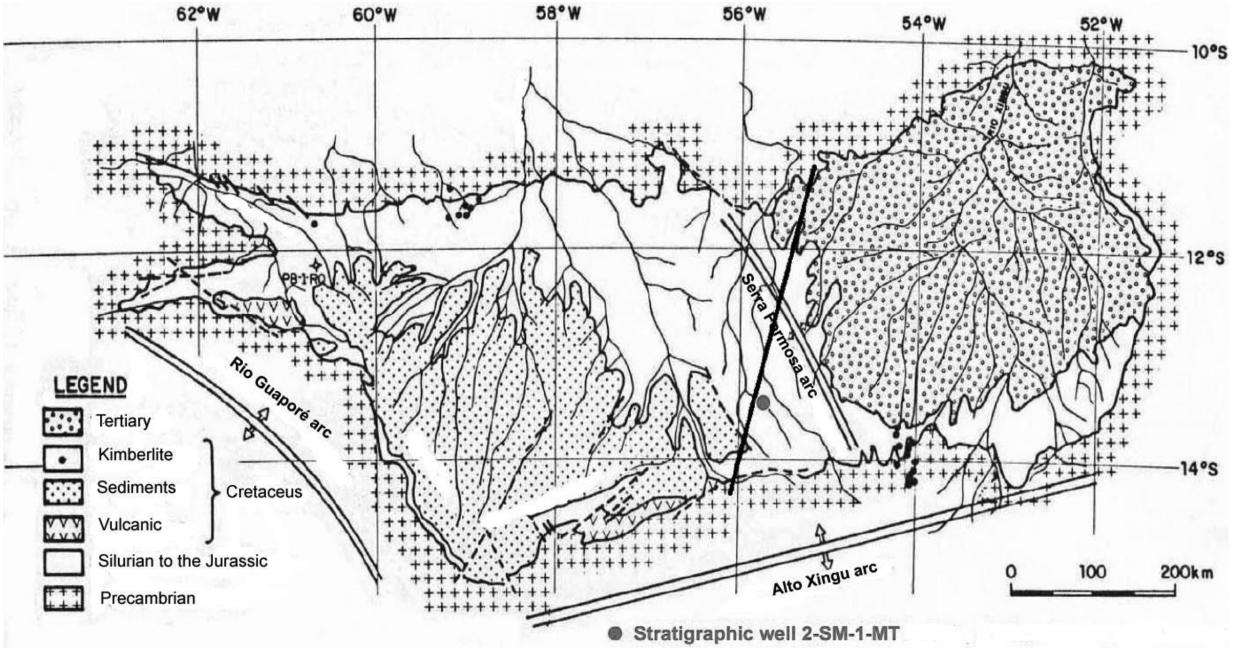

Figure 2 – Geological map of the Parecis Basin (Siqueira, 1989).

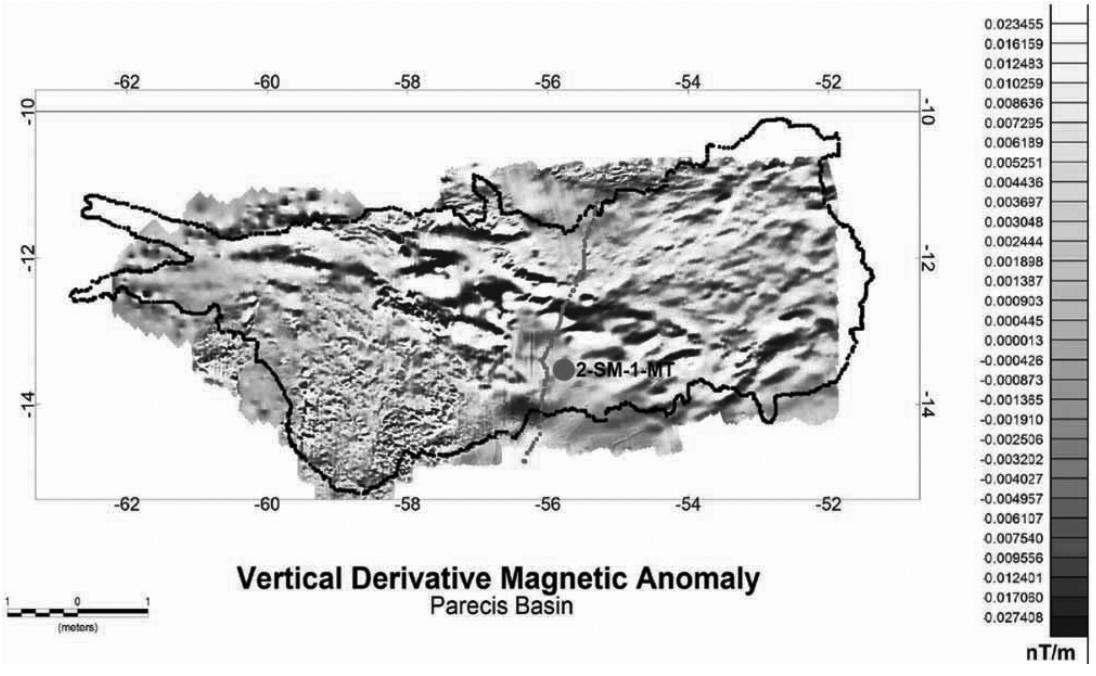

Figure 3 – Map of the vertical derivative of the magnetic anomaly in the Parecis Basin. This technique gives information about the magnetic lineaments.

where $\mathbf{R}$ is a rotation matrix and $\mathbf{C}$ is a real telluric distortion tensor which is itself the product of three tensors

$$\mathbf{C} = g\mathbf{TSA} \tag{6}$$

g is a scaling factor ("site gain"), $\mathbf{T}$, $\mathbf{S}$ and $\mathbf{A}$ are called *twist*, *shear* and *anisotropy*, respectively. The factor g and anisotropy $\mathbf{A}$ form together the indeterminable part of $\mathbf{C}$ which is absorbed into the regional impedance, $Z_{\text{regional}} = g\mathbf{AZ}_{2D}$. The *twist* tensor, $\mathbf{T}$, and the *shear* tensor, $\mathbf{S}$, are the determinable parts of $\mathbf{C}$. $\mathbf{T}$ rotates clockwise the electric field produced by $\mathbf{SAZ}_{2D}$ through the *twist* angle $\arctan(t)$ and $\mathbf{S}$ develops anisotropy on an axis which bisects the regional induction

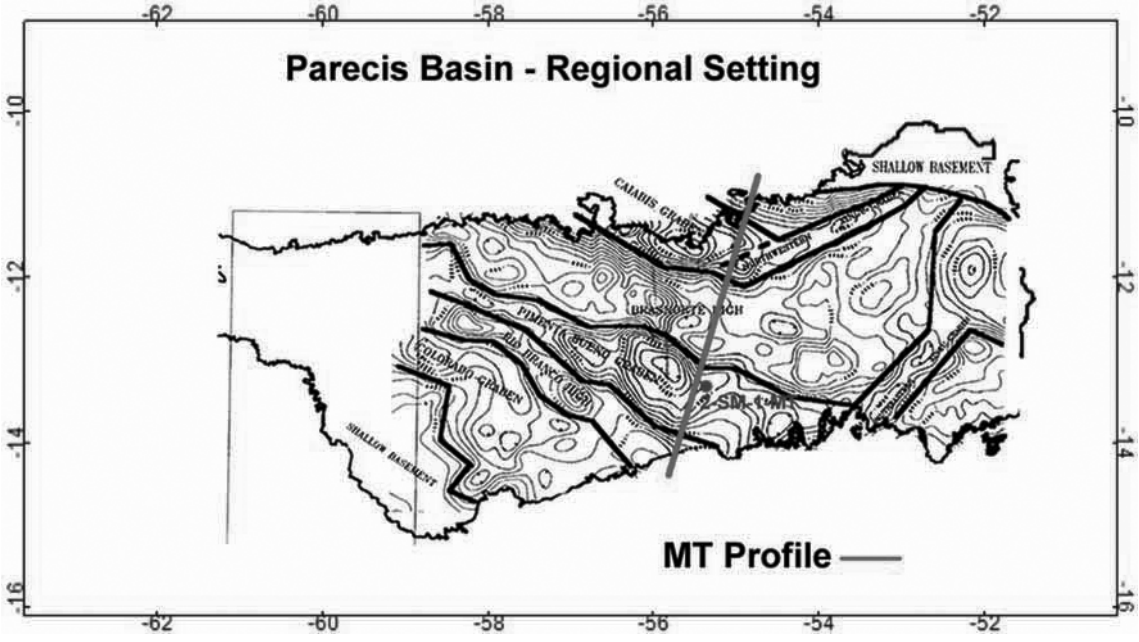

Figure 4 – Three-dimensional modeling of the geometry of the Parecis Basin obtained through gravimetric data (Braga & Siqueira, 1995).

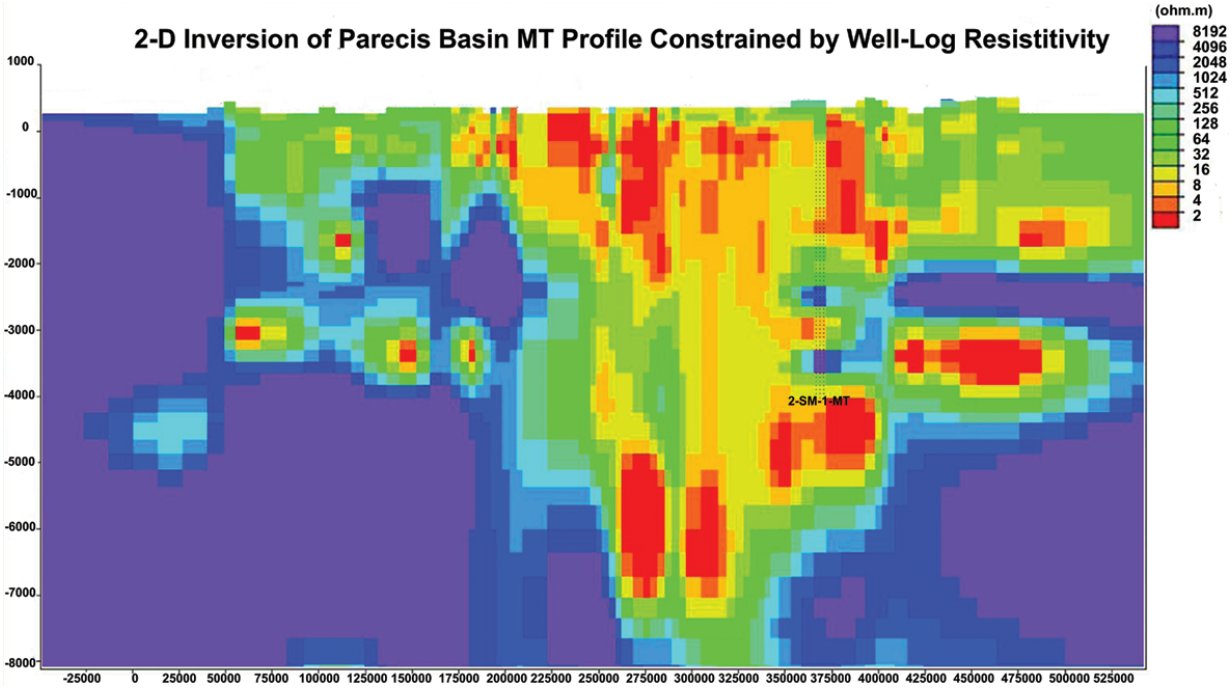

Figure 5 – 2-D inversion of MT data of the Parecis Basin profile (constrained by well-log resistivity data) performed using a routine developed by Rodi & Mackie (2001). Inversion allows to estimate the distribution of conductivity.

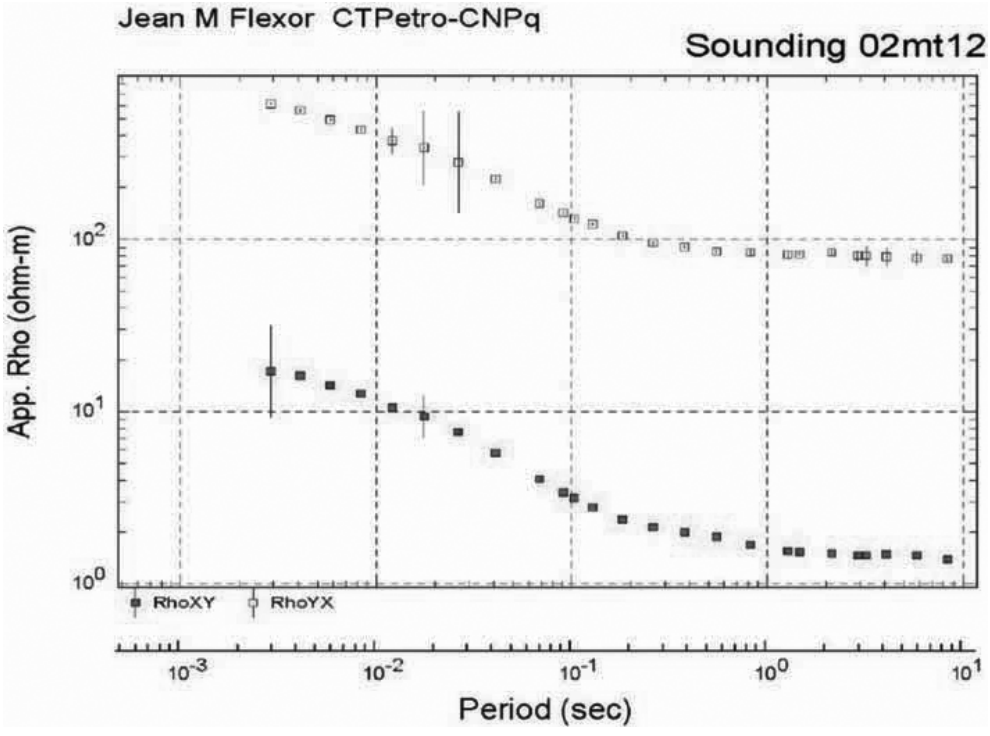

Figure 6 – Vertical displacement among the curves of apparent resistivity regardless of frequency in MT sounding with static shift (MT station 02mt12).

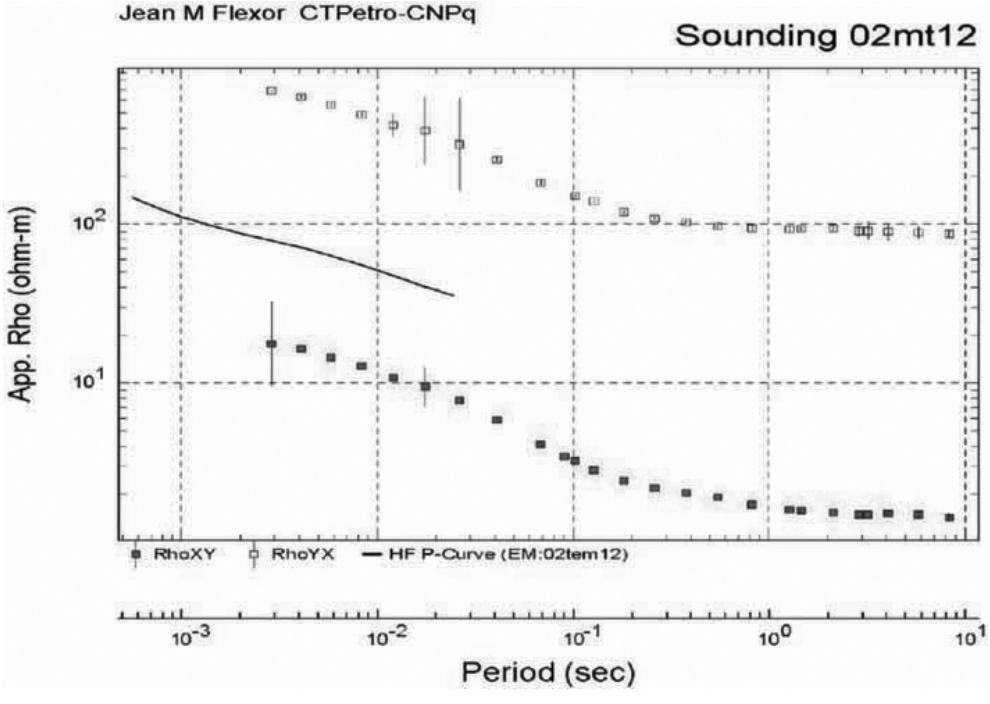

Figure 7 – TDEM resistivity measurement: a tool for static shift correction. The TDEM method is not affected by distortions, because it uses magnetic fields to study geoelectric properties.

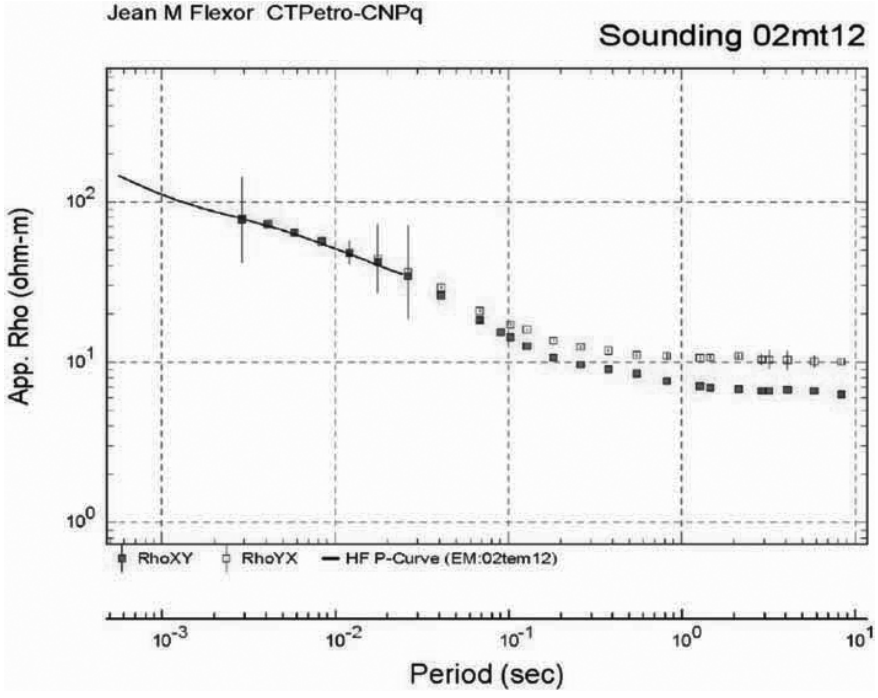

Figure 8 – Static shift correction (MT station 02mt12). Curves MT must be moved vertically to coincide with TDEM ones.

principal axes, rotating a vector by the *shear* angle, $\arctan(e)$. The observed impedance expressed with the Groom-Bailey factorization becomes (Groom & Bailey, 1989):

$$\tilde{\mathbf{Z}}_{\text{obs}}(\theta_0) = \mathbf{RTS}\tilde{\mathbf{Z}}_{\text{regional}}\mathbf{R}^{\mathbf{T}}$$

$$= \begin{pmatrix} \cos\theta & -\sin\theta \\ \sin\theta & \cos\theta \end{pmatrix} \begin{pmatrix} 1-te & e-t \\ e+t & 1+te \end{pmatrix} \qquad (7)$$

$$\times \begin{pmatrix} 0 & A \\ -B & 0 \end{pmatrix} \begin{pmatrix} \cos\theta & \sin\theta \\ -\sin\theta & \cos\theta \end{pmatrix}$$

The necessity of the four independent parameters in the distortion tensor factorization is illustrated in Figure 9 (Groom & Bailey, 1989), which shows a scenario where the MT data are collected at the centre of an elliptical highly conductive surface region, encompassed by an insulating substratum in a moderately conductive region. This highly conductive surface region causes the telluric currents to be twisted to its local strike. This clockwise rotation of the telluric vectors is contained in the twist tensor, $\mathbf{T}$. There is also splitting of the principal impedances with different stretching factors. This anisotropic effect is contained in the anisotropy tensor, $\mathbf{A}$. Meanwhile, the shear tensor, $\mathbf{S}$, stretches and deflects the principal axes so that they no longer lie orthogonal to each other. Whereas $\mathbf{A}$ does not change the directions of the telluric vectors lying along either of the principal axes, $\mathbf{S}$ generates the maximum angular deflection along these principal axes.

DETERMINATION OF THE STRIKE ANGLE

Following the above procedures, we obtained frequency independent estimates of the *twist*, *shear* and regional *strike* for a set of 36 soundings stations from the MT profile using the *strike* 4.1 program of McNeice & Jones (2001). These estimates can be found over a sufficiently wide band of frequencies. This is done by constraining iteratively the *twist*, *shear* and *strike* in order to find a frequency band where the misfit error is acceptable. We apply a four-steps procedure: i) an unconstrained decomposition whose distortion parameters were allowed to vary freely ($-45° < \textit{shear} < 45°$), ($-60° < \textit{twist} < 60°$) and ($-360° < \textit{strike} < 360°$); ii) we constrain the *twist* angle to its median value for a representative frequency range and we repeat the decomposition procedure; iii) the *twist* constrained data show generally an improved stability in shear, then we constrain the *shear* angle to its median value over a representative frequency range and repeat the decomposition procedure; iv) if the *twist* and *shear* constrained data result in a stability in *strike* angle over a representative period range, we constrain the *strike* angle to its median value and we repeat the decomposition procedure, to obtain, finally, individual *strike* angles for each MT station. An

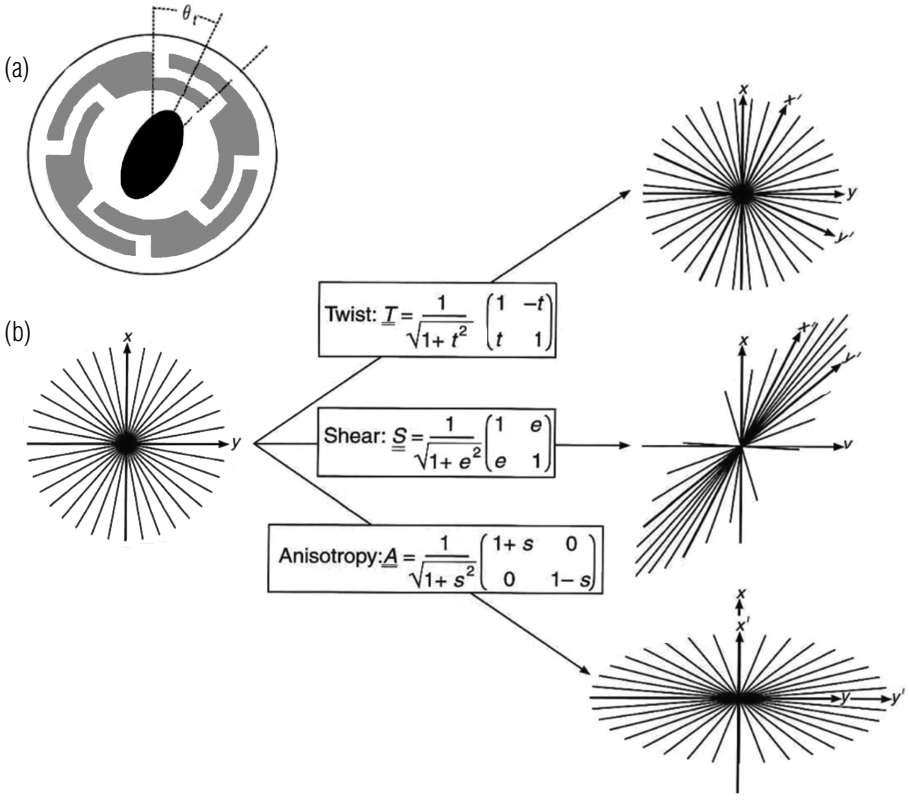

Figure 9 – (a) A scenario in which MT data are collected at the centre of a conductive swamp (black) that is encompassed by a moderately conductive region (grey), and an insulator (white). B_t denotes the local strike of the swamp, which 'twists' the telluric currents. The anomalous environment also imposes shear and anisotropy effects on the data; (b) Distortion of a set of unit vectors by *twist* **T**, *shear* **S**, and *anisotropy* **A**, operators, which are parameterized in terms of the real values t, e and s, respectively (Groom & Bailey, 1989).

example plot of (a) unconstrained, (b) shear constrained, (c) twist constrained and (d) fully constrained distortion parameters to the sounding stations MT-22 is shown in Figure 10.

In order to verify if an average geoelectric strike can be compatible with the basin's geological strike, a procedure of decomposition of MT impedance tensor (McNeice & Jones, 2001) for a set of 36 MT soundings along the profile was applied. The strike angles obtained by each of the MT stations can be seen in Figure 11.

An angle distribution of geoelectric strike is shown in the histogram of Figure 12.

DISCUSSION AND CONCLUSIONS

The determination of the regional strike in the presence of noise and galvanic distortion can lead to instability in decomposition procedures. This occurs to the sounding stations 02mt46, 02mt61, 03mt12 and 02mt15 where the decomposition analysis failed because the shear angles were very near to $\pm 45°$. In these cases, the decomposition models became underdetermined. In order to recover the regional impedances, we use the strike found in adjacent stations or other independent information (like geological strike). The inherent $\pi/2$ ambiguity of the strike determination (Eq. 4) was solved by using the tipper strike (Eq. 4a).

In most of the soundings, the average period range adopted as representative of stability in the strike angle was 0.05-10 sec. The behavior of the strike angle along the profile is not uniform as expected.

Each vector in Figure 11 represents the direction of the local geoelectrical strike obtained from the Groom Bailey decomposition (Strike Program, McNeice & Jones). The image of Figure 12 is a histogram which shows statistically the predominant directions. The results show that the distribution of the strike angles is not uniform as expected, but the strike direction assumed *a priori* is compatible with the mean strike angle directions. These directions are representative of the whole frequency range measured in each station. Further, researches could include the study of various frequencies that probably would provide different results.

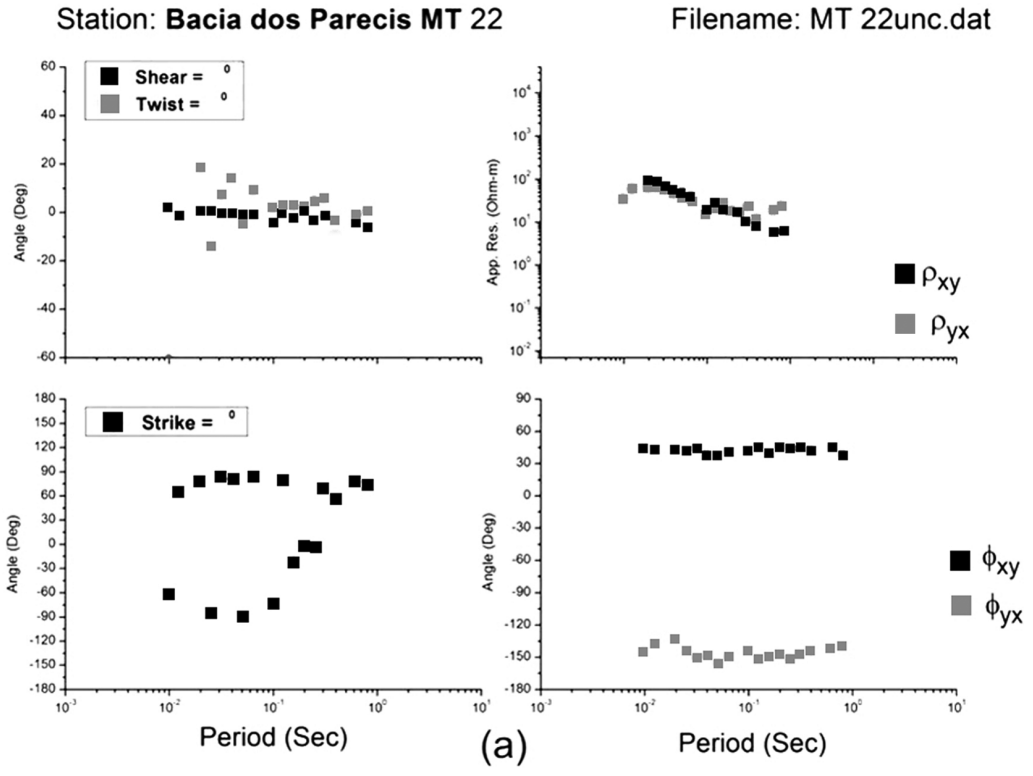

Figure 10a – Plot of fully unconstrained distortion parameters of the impedance tensor to the sounding station MT-22.

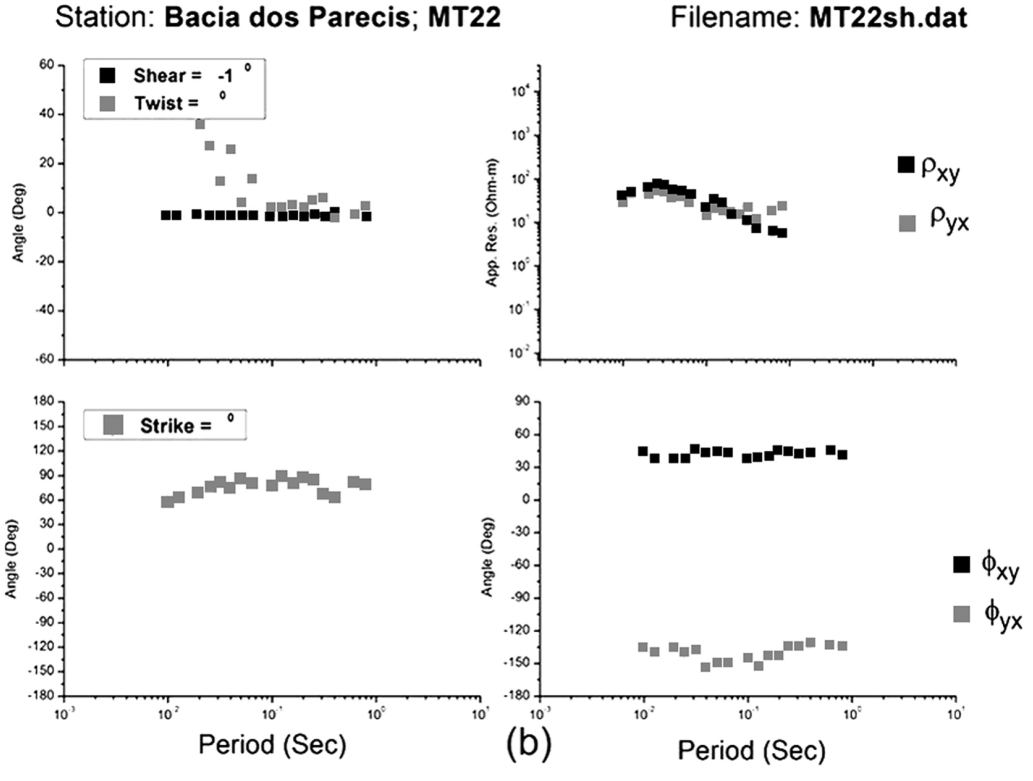

Figure 10b – Plot of shear constrained distortion parameters of the impedance tensor to the sounding station MT-22.

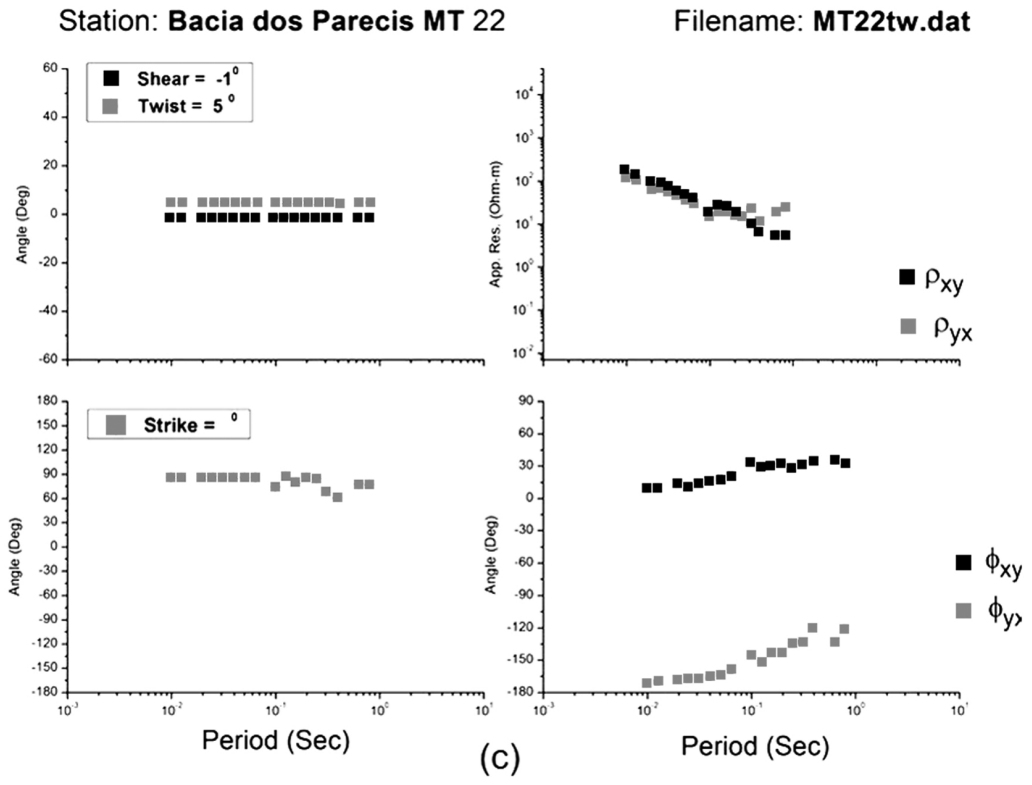

Figure 10c – Plot of shear constrained and twist constrained distortion parameters of the impedance tensor to the sounding station MT-22.

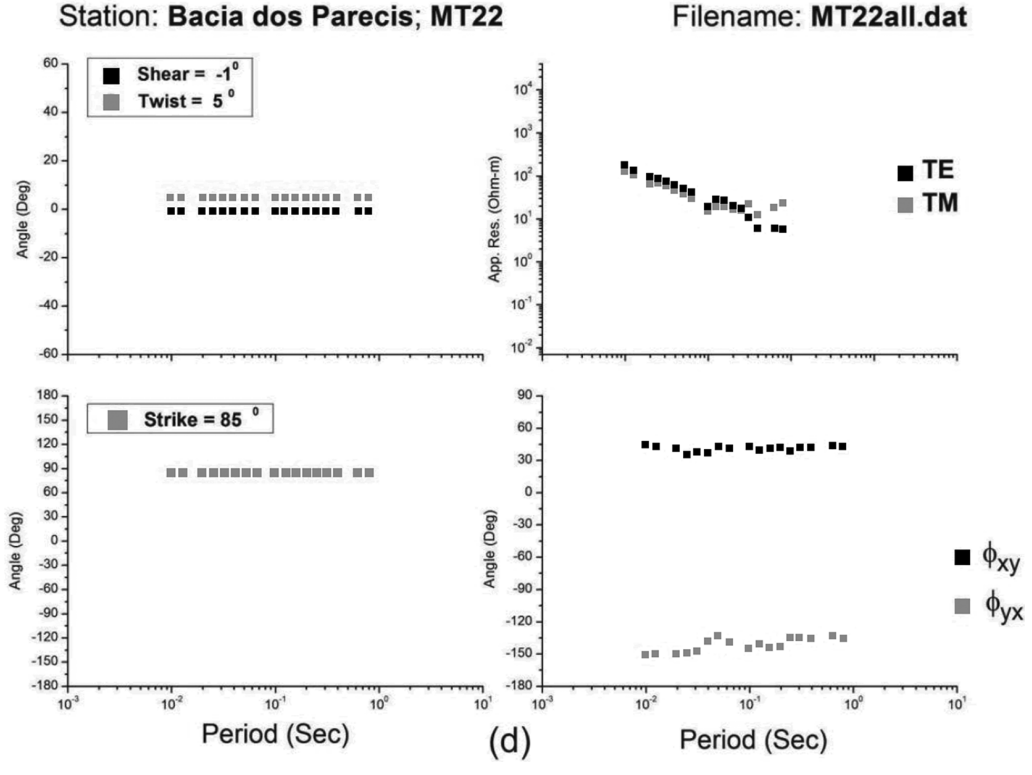

Figure 10d – Plot of fully constrained distortion parameters of the impedance tensor to the sounding station MT-22.

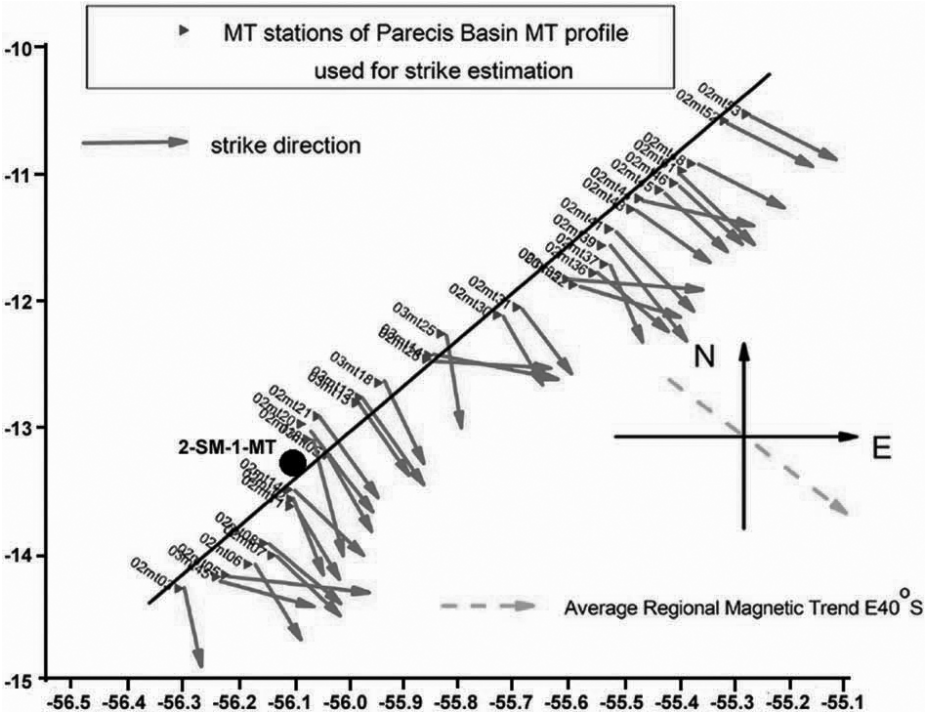

Figure 11 – Geoelectric strike directions (arrows) estimated at selected sounding stations of the Parecis Basin MT profile.

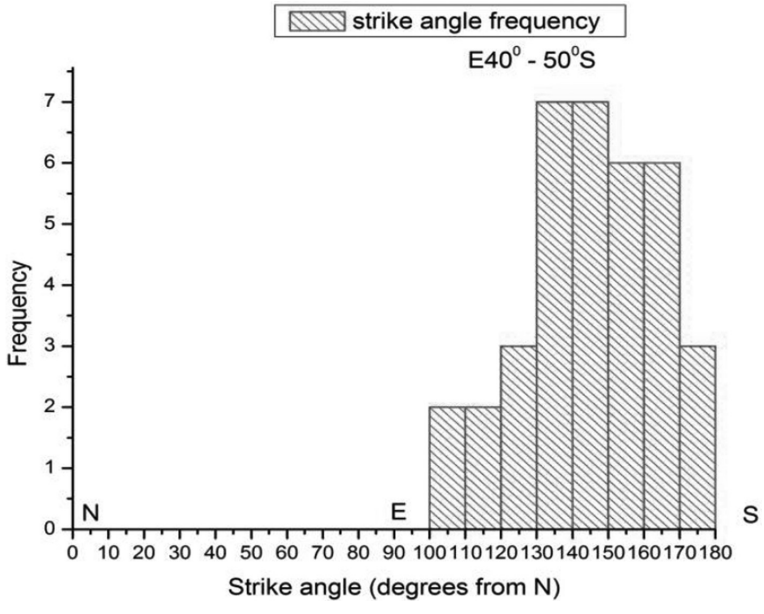

Figure 12 – Histogram of the estimated geoelectric strike angles with an angular predominance around 130° and 140°.

The geological strike direction assumed in the 2-D inversion, before the decomposition of the MT impedance tensor is compatible with the mean calculated strike directions (Fig. 6). This can be observed in the central part of the map from the vertical derivative of the magnetic anomaly (Fig. 3) and the tectonic model obtained by the inversion of gravity data (Braga & Siqueira, 1995) (Fig. 4). Our knowledge of the tectonic features of the Parecis Basin comes from a three-dimensional model of the basement topography based on downward continuation of gravity field constrained by spectral estimates of depth to magnetic

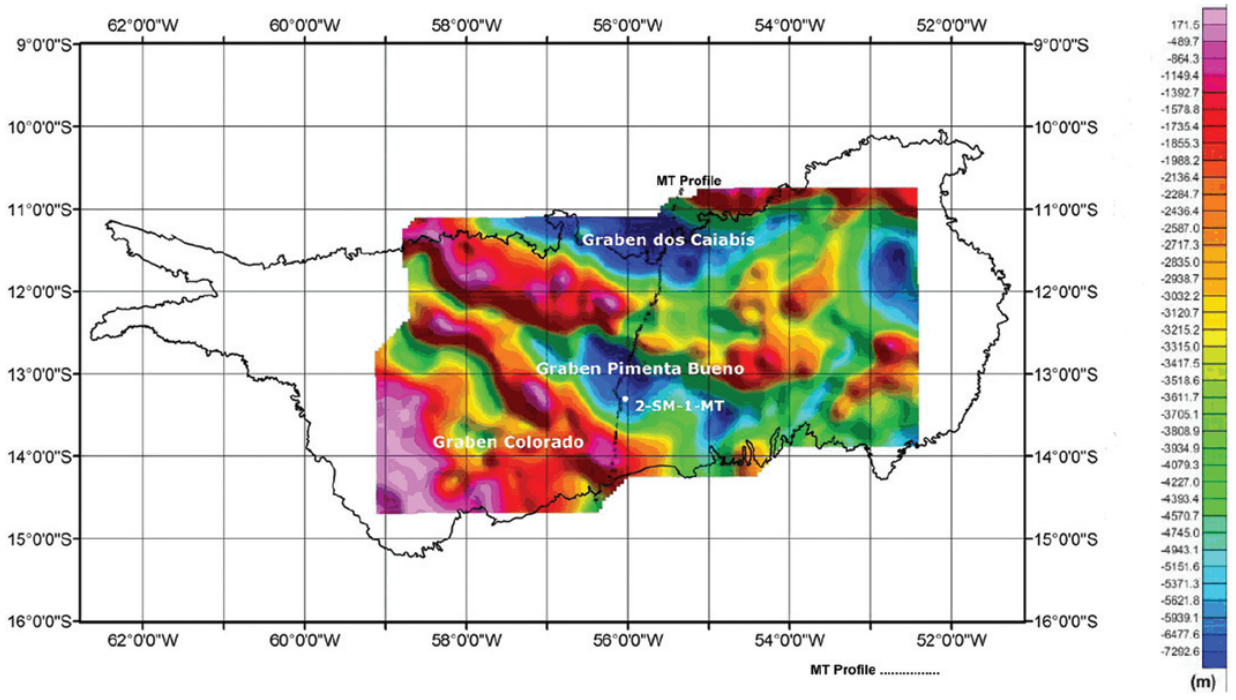

Figure 13 – 3-D gravity modeling of the basement topography beneath the Parecis Basin and the main tectonic features (Braga & Siqueira, 1995). The MT profile across the basin and the exploratory well 2-SM-1-MT are shown.

sources (Braga & Siqueira, 1995). The variations observed of the geoelectric strike angle value can be related to the geotectonic structures of the Parecis Basin and their influences in the geoelectric anisotropy. We can suppose that the most regular strike angles distribution correspond to the deepest sedimentary structures: Caiabis, Pimenta Bueno and Colorado grabens (Fig. 13). In the interface regions we can expect a geoelectric anisotropy which distorts the regional impedance tensor.

REFERENCES

BRAGA LFS & SIQUEIRA LP. 1995. Three-Dimensional Gravity Modeling of the Basement Topography beneath Parecis Basin, Brazil. In: Proceedings of the 5th Latin American Petroleum Congress, Rio de Janeiro, Brazil, 1995, 1–5.

GROOM RW & BAILEY RC. 1989. Decomposition of magnetotelluric impedance tensors in the presence of local three-dimensional galvanic distortion. Journal of Geophysical Research, 94: 1913–1925.

McNEICE GW & JONES AG. 2001. Multisite, multifrequency tensor decomposition of magnetotelluric data. Geophysics, 66(1): 158–173.

RODI W & MACKIE RL. 2001. Nonlinear conjugate gradients algorithm for 2-D magnetotelluric inversion. Geophysics, 66(1): 174–187.

SIQUEIRA LP. 1989. Bacia dos Parecis. Boletim de Geociências da Petrobras, Rio de Janeiro, 3(1/2): 3–16.

STERNBERG BK, WASHBURNE JC & PELLERIN L. 1988. Correction for the static shift in magnetotellurics using transient electromagnetic soundings. Geophysics, 53: 1459–1468.

VOZOFF K. 1991. The Magnetotelluric Method. In: NABIGHIAN MN (Ed.). Electromagnetic Methods in Applied Geophysics. Vol II. Soc. Expl. Geophysics, p. 641–711.

NOTES ABOUT THE AUTHORS

Hans Schmidt Santos is a Ph.D. student in Geophysics at the Observatório Nacional Postgraduate Program in Rio de Janeiro. His areas of interest are electromagnetic methods applied to Geophysics.

Jean Marie Flexor is a retired researcher of the Observatório Nacional in Rio de Janeiro. In 1971 he coordinated the nuclear geophysical laboratory at Universidade Federal da Bahia. Since then, he has advised many M.Sc. and Ph.D. students in Geophysics and has conducted geophysical research in nuclear and electromagnetic methods.